

Are magnetic resonances practical transport controllers in fusion plasmas? The TJ-II experience

D López-Bruna¹, V I Vargas² and J A Romero¹

¹ Laboratorio Nacional de Fusión, Ciemat, Madrid, Spain

² Plasma Laboratory for Fusion Energy and Applications, Cartago, Costa Rica

daniel.lopezbruna@ciemat.es

Abstract. The TJ-II stellarator is a mid-size Helic design (high rotational transform, low magnetic shear) that allows for external control of the rotational transform profile. The long experience with locating diverse magnetic resonances at different plasma radii has assessed their reliability as transport controllers: in low density electron cyclotron heating plasmas, a “transport barrier effect” is found in most of the confinement zone accompanying magnetic resonances; in higher density and beta plasmas under neutral-beam heating operation, resonant layers show a clear incidence on the access to the H-mode of confinement or, likewise, on the back transition to L-mode. Moreover, confinement events similar to tokamak phenomenology have been also related with magneto-hydrodynamic activity around the magnetic resonances and are, consequently, amenable to external control. All in all, the TJ-II experience posits magnetic resonances as natural transport and stability controllers in toroidal plasmas. Further studies must either confirm or set operational limits to these findings.

1. Introduction

In toroidal magnetic confinement the geometry implies that some twisting (winding number) of the magnetic field lines is necessary to short-circuit charge separation due to curvature drifts. Magnetically resonant layers are regions where the magnetic field lines, owing to their ability to close on themselves after a few turns around the toroid, can break locally the ideal toroidal nesting of flux surfaces. This breaking of the topology of the magnetic field starts with resonant flux surfaces that are linearly unstable and give rise to volumes with cross sections that resemble islands; hence the close relationship between magnetic resonances and magnetic islands. Because of this, considerable effort was paid in early studies on stellarator confinement to the question of particle containment within the plasma volume. Using electron guns or other means to check for orbit containment, a fine structure of containment time was found in relation with the rotational transform: particles would get confined for a long time in some places, while being easily lost in very close locations supposedly associated with low order rational values of the rotational transform (magnetic resonances); see, for instance, stellarator papers in [1]. Later, in the nineties, these magnetic resonances were confirmed to have a locally deleterious effect on confinement; however, and since lowest order rational values are “isolated” in terms of density of low order rational values, magnetic resonances in the confining volume are generally sided by robust flux surfaces with good particle containment properties. As a consequence, it was proposed that magnetic resonances must either be avoided working with very low magnetic shear (small radial variation of the rotational transform) or included with high enough magnetic shear so that the resonant regions are very narrow [2]. Results have accumulated in the early 2000’s proving that



transport can be also significantly reduced at, or beside, magnetically resonant locations. To cite a few examples, reductions of transport in the O-point of magnetic islands have been identified in LHD [3] and rational surfaces were found to possibly play an important role in the formation of internal barriers in high electron temperature stellarator/heliotron plasmas [4,5]. Further indication that magnetic resonances need not be detrimental for confinement is the well-known relation between the effect on L-H transition quality and the edge value of the rotational transform [6,7,8]. Finally, let us recall that the importance of magnetic resonances in the formation of transport barriers is also supported by many results from tokamaks (e.g. DIII-D [9], JET [10] to cite some). It looks like no theory of toroidal magnetic confinement for fusion applications would be complete without an assessment of the role of resonant regions inside the confining volume.

This work is based on the experience accumulated with the TJ-II stellarator, a machine with $\sim 1 \text{ m}^3$ plasma volume immersed in $\approx 1 \text{ T}$ magnetic fields. It is a mid-size Helic design (high rotational transform, low magnetic shear) with the notable property of allowing for external control on the rotational transform profile over a wide range of values and forms. This capability has been exploited to investigate the role of magnetic resonances on confinement properties. In rough numbers, the device produces plasmas with densities in the range $0.5\text{--}5.0 \cdot 10^{19} \text{ m}^{-3}$, corresponding electron temperatures $1\text{--}0.2 \text{ keV}$ and ion temperatures in the 0.1 keV range. Typical working gas is hydrogen and the heating systems are Electron Cyclotron Resonance (up to 0.6 MW) and Neutral Beam Injection (about 1.2 MW with two opposing tangential injectors). This work is a quick overview of results (Section 2) from the perspective of confinement control, which we summarize in Section 3.

2. TJ-II phenomenology

As pointed above, in terms of heating and fuelling there are two broad types of plasma produced with the TJ-II device. Low density ($< 10^{19} \text{ m}^{-3}$) and high T_e ($\sim 1 \text{ keV}$) correspond to ECR plasmas. NBI plasmas have much more coupled electron and ion species and densities normally well above 10^{19} m^{-3} ; the density is more difficult to maintain in steady state and, other conditions fixed, is very dependent on the wall conditioning. The response of most diagnostics is different depending on the plasma type, ECR or NBI. For these reasons the results are presented according to the heating/fuelling type.

2.1. Low density ECR heated plasmas

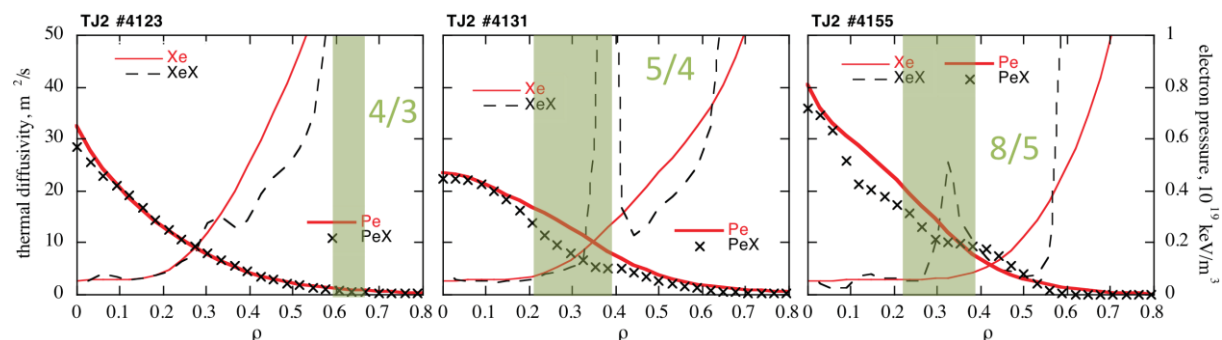


Figure 1. Profile of Thomson Scattering electron pressure (crosses) and χ_e from transport balance (dashes) for three ECR heated TJ-II discharges in magnetic configurations with resonances occupying approximately the shaded radial region. Corresponding smooth profiles from transport modelling are also shown (lines)

The effects of magnetic resonances in transport and stability have always been a matter of interest in TJ-II experiments. A systematic study about local effects due to the magnetic resonances was initiated in 2003 with the idea of clarifying the role of magnetic resonances in global transport scalings [11]. This motivated performing balance analysis based on Thomson Scattering data for the electron density and temperature profiles in different magnetic configurations. An example is shown in figure 1, where

the experimental electron pressure is shown (crosses) along with the corresponding experimental electron heat diffusivity (χ_e , dashed line) for three discharges in configurations that have different magnetic resonances inside the plasma. χ_e is defined in a standard way considering the local net heat flux, electron density and electron temperature gradient scale-length. Shaded rectangles in the figures indicate the approximate location of the labelled resonances. A transport model was used to find steady states that approach the experimental electron pressure profiles (solid lines), although such features as a flattening in the electron temperature profile cannot be obtained unless some specific ingredient is included in the models.

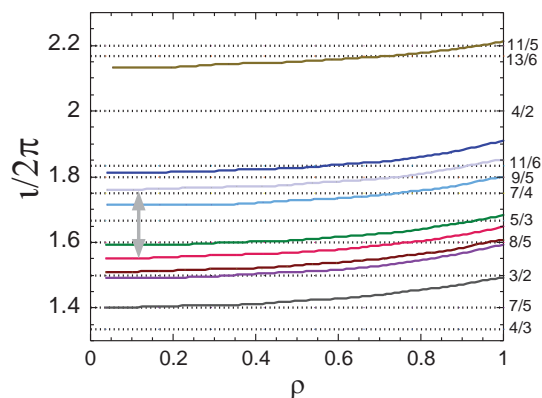


Figure 2. Vacuum rotational transform profiles calculated for different magnetic configurations of the TJ-II Helic. Horizontal dashed lines with corresponding labels in the right axis indicate low-order rational values of $\nu/2\pi$. The crossings with the profiles mark the locations in plasma minor radius around which the magnetic resonances are expected to occur. A double arrow indicates the span of the magnetic configuration scan in figure 3.

From the results shown in figure 1 it would seem that occasional flattenings in the electron pressure profiles are due to the presence of magnetic resonances. Many more cases were analysed in this way [12] using data from configurations characterized by the vacuum $\nu/2\pi$ values shown in figure 2, but no systematic pattern was found: the eventual occurrence of flattenings may or may not be coincident with the expected location of the resonances, pointing to artifacts after fitting to the Thomson Scattering profiles. Bootstrap current density profiles were not expected to be important in these discharges with net plasma currents in the ~ 1 kA range. This called for a more systematic study where the magnetic configuration scan could be done in small steps, so as to place a certain resonance, say $\nu/2\pi = 8/5$, in nearby locations from one configuration to the next.

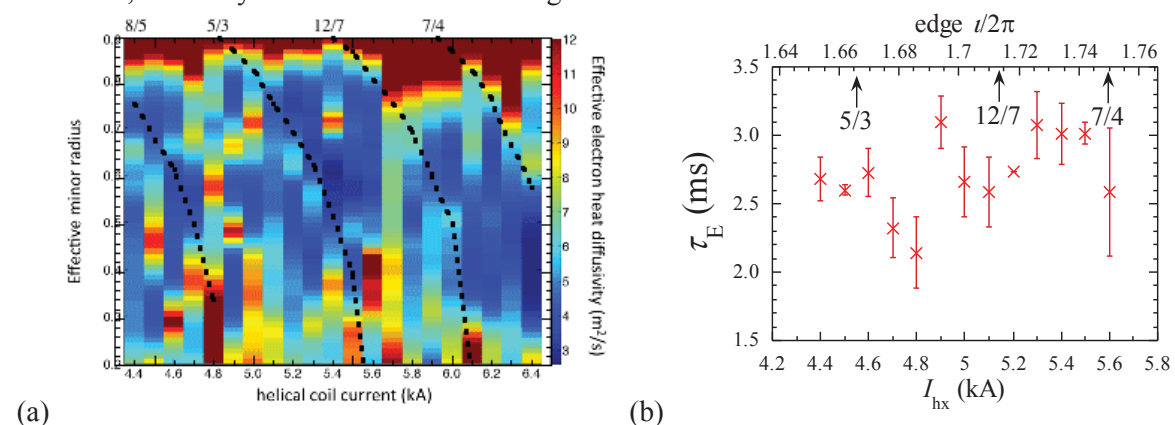


Figure 3. (a) Contour plot of χ_e -profiles (color bar at right side) for different magnetic configurations characterized by their current in the helical conductor, I_{hx} . Dotted lines indicate the location of the main magnetic resonances (labelled on top). (b) Energy confinement times from balance calculations corresponding to some of the configurations shown in panel (a), as indicated with the I_{hx} values. Error bars are the standard deviation from repetition discharges in each configuration.

Figure 3 (a) is a contour plot of effective electron thermal diffusivities (see values in color bar) obtained from a fine magnetic configuration scan covering, with 21 interleaved configurations, the

range indicated with a double arrow in figure 2. Dotted lines indicate the “path” followed on minor radius (left axis) by the main vacuum magnetic resonances (labelled on top) along this scan. Abscissa values are the electric current in the helical conductor of the device, I_{hx} , which provides most of the rotational transform in TJ-II configurations and serves as an appropriate label for the scan.

The results in figure 3 (a) were obtained after averaging repetition discharges for every magnetic configuration. The analysis of such experiments [13] strongly suggested a different view of how magnetic resonances affect confinement: they can be placed essentially anywhere in the plasma despite the low magnetic shear of TJ-II plasmas and, systematically, larger temperature gradients accompany them as if a kind of barrier moved along. Of course, a precise location of the magnetic resonances is not known in these experiments. Thus, the path followed by the resonances in figure 3 (a) corresponds to vacuum locations and here we can only claim that lower electron heat transport *follows* the resonances, but maybe beside them. Additionally, the experiments warned about the interpretation of rotational transform scalings for stellarators. Figure 3 (b) shows the average electron energy confinement time (τ_E , radiation not considered in the balance) for a part of the scan shown in figure 3 (a) as noted in the I_{hx} values. A fine structure, which somehow reminds one about old results in particle containment studies, seems to appear. The error bars in τ_E are standard deviations from repetition discharges, which unfortunately cannot account for all the uncertainties in the analysis. Despite this, the results of figure 3 (b) would be rather incomplete without the help of figure 3 (a).

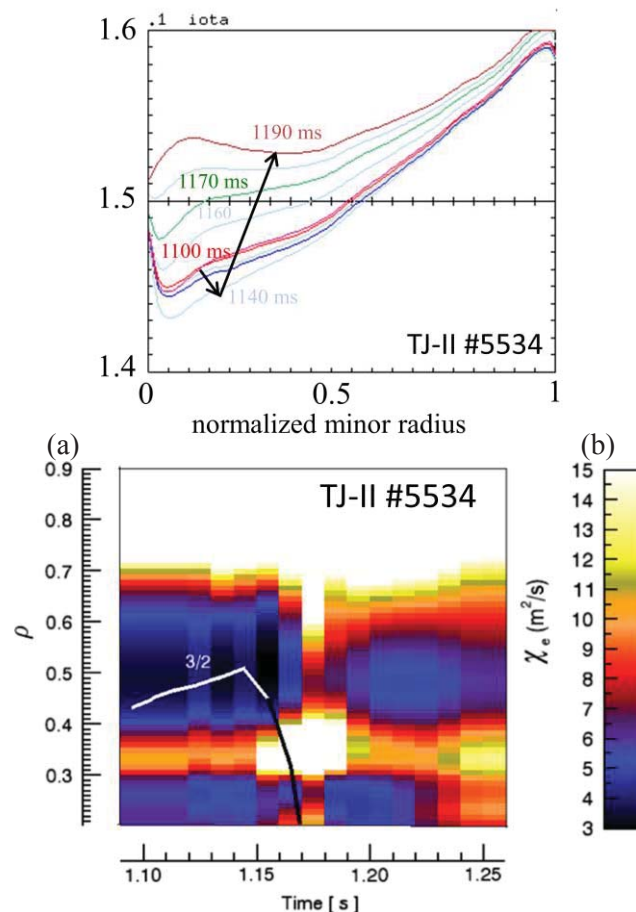


Figure 4. Time evolution of (a) the calculated rotational transform and (b) the electron diffusivity profiles obtained from heat balance, for a discharge with double ramp in the ohmic transformer.

Another motivation for these studies stemmed from the knowledge that, in discharges with increased (negative) magnetic shear via ohmic induction, the simultaneous inclusion of several resonant layers

within the plasma volume was compatible with improved confinement [11,14]. This result was well in line with W7-AS results [2], according to which the larger magnetic shear caused by the ohmic current would improve confinement. It was likewise possible to identify a so-called “signature”, or characteristic evolution of the plasma signals due to the appearance and movement of the resonant layers throughout the plasma [15]. This systematic behavior suggested looking for the effect of resonant layers on transport by tracking them with the effective heat diffusivities —or, almost equivalently, the inverse gradient scale-lengths— during discharges with ohmic induction. Not surprisingly, the same “transport barrier effect” was found in most of the confinement zone [16] rather independently of the magnetic shear unless it was forced to be practically zero over a wide radial region [17] as figure 4 shows. There we see the calculated evolution of the rotational transform for a discharge with ohmic induction. Initially ($1100 \text{ ms} < t < 1140 \text{ ms}$) a negative current is induced, which increases the magnetic shear. Then the current ramp in the primary of the transformer is inverted provoking the induction of positive currents and an increment in $i/2\pi$, especially in the hotter plasma core. This process tends to force minima in the rotational transform profile. The resonance $3/2$ initially present in the configuration disappears from the confining volume at approximately $t \approx 1180 \text{ ms}$. The calculations of $i/2\pi$ cannot be accurate at this point because the flux surface coordinates are no longer a good geometrical description. However, the transport balance analysis (figure 4 (b)) clearly reflects a pronounced flattening of profiles, manifested in a very high χ_e . Interestingly, before that happens, a most prominent resonance like $3/2$ is related with *lower* electron heat diffusivities (note the contour plot values around the resonant location for $t < 1160 \text{ ms}$).

The results shown in figure 3 (a) were obtained on a shot-to-shot basis using Thomson Scattering as the main diagnostic tool, while dynamic results like figure 4 (b) were based on Electron Cyclotron Emission to allow for a practically continuous evolution of the T_e -profile. The TJ-II capability of working with variable configuration discharges [18,19,20] at close-to-vacuum magnetic shear was later used to reproduce the results of figure 3 (a) in one single discharge. The two discharges in figure 5 correspond to dynamic configuration scans where the offset of the rotational transform decreases (a) or increases (b), thus forcing respectively a movement outwards or inwards of the main resonances (see figure 1) through minor radius. These ECR plasmas are initiated around $t = 1040 \text{ ms}$ and the evolution of the net plasma currents can distort the vacuum paths (lines) of the resonances. However, the qualitative similarity with figure 3 (a) is clear: the presence of magnetic resonances does not necessarily deteriorate global confinement because they have local effects that are, as suggested in particular cases like the CERC [4], related with zones of reduced χ_e .

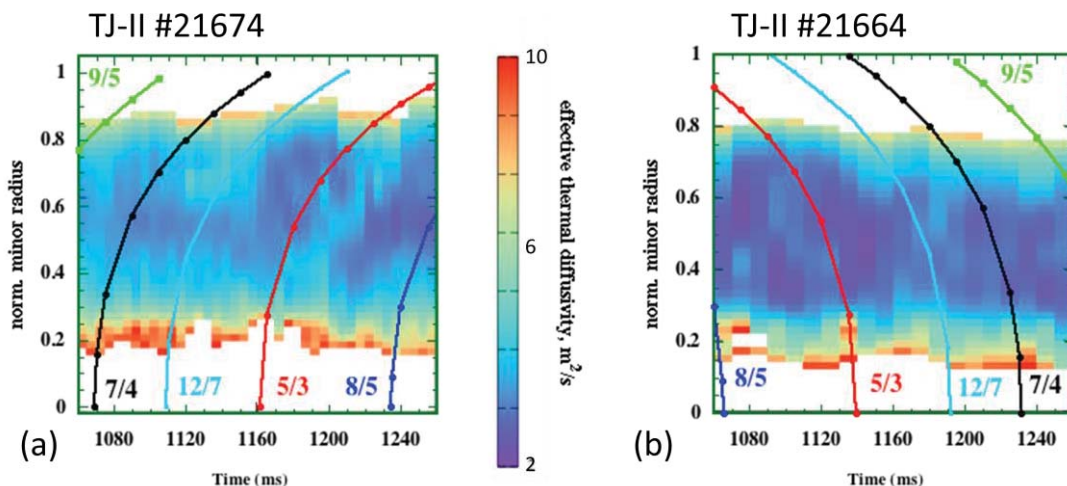


Figure 5. Contour plot of electron thermal diffusivity profiles from transport balance for two discharges with (a) downwards and (b) upwards sweepings of the rotational transform profile, which respectively cause outwards and inwards movements of the vacuum magnetic resonances through

plasma radius (lines).

The results shown up to here demanded a thorough investigation of possible causes leading to these local changes in confinement. In summary, associated with magnetic resonances, it was verified that there are local changes in plasma potential (edge electric probes) and rotation of density fluctuations (Doppler reflectometry) that convey considerable $\sim 10^5 \text{ s}^{-1} \text{ ExB}$ flow shear. The reason why this happens is unclear despite the plausibility of some explanations. For example, the existence of the resonant regions can couple parallel and radial transport thus favoring the outwards movement of the fastest species (electrons in these cases), which would imply a tendency to electron-ion flow unbalance and the corresponding establishment of a locally strong radial electric field [21,22,23].

2.2. NBI plasmas

The studies on how magnetic resonances affect the plasma operation were extended to higher density and beta plasmas under NBI heating operation. Resonant layers were known to have a clear incidence on the access to the H-mode of confinement, thus defining “windows” in H-mode quality—or even existence—depending on the edge rotational transform [8], well in line with other stellarator devices. It was also found that, around the maximum (negative) pressure gradient region, the changes in perpendicular velocity shear depend on what magnetic resonance is placed in the region [24]. NBI plasmas do not allow for ECE measurements due to the large densities so we cannot track the presence of resonances in a way similar to the one presented for ECR plasmas. However, the technique of variable configuration discharge was once more used to provide cause-effect experiments. In this case the question was whether a magnetic resonance properly placed in the plasma could cause a transition; or, also importantly, whether it could also withdraw the plasma from the H-mode just by retiring from such appropriate plasma region. Effectively, by sweeping different magnetic resonances through NBI plasmas it was confirmed that magnetic resonances alter confinement in a sharp way (resembling typical L-H transitions) once they reach certain radial location in the main gradients zone; but such “transitioned” state disappears as the configuration change proceeds further [23]. This was proposed as a potentially powerful tool for plasma confinement control: if these results remain valid in reactor-grade plasmas, a reactor design able to move (just slightly) magnetic resonances along the plasma minor radius could have external control on the access to and from the H-mode of confinement. This is easy to conceive for a stellarator design, but also tokamaks would benefit just at the expense of using appropriate transformer control techniques [25] or other means of current drive.

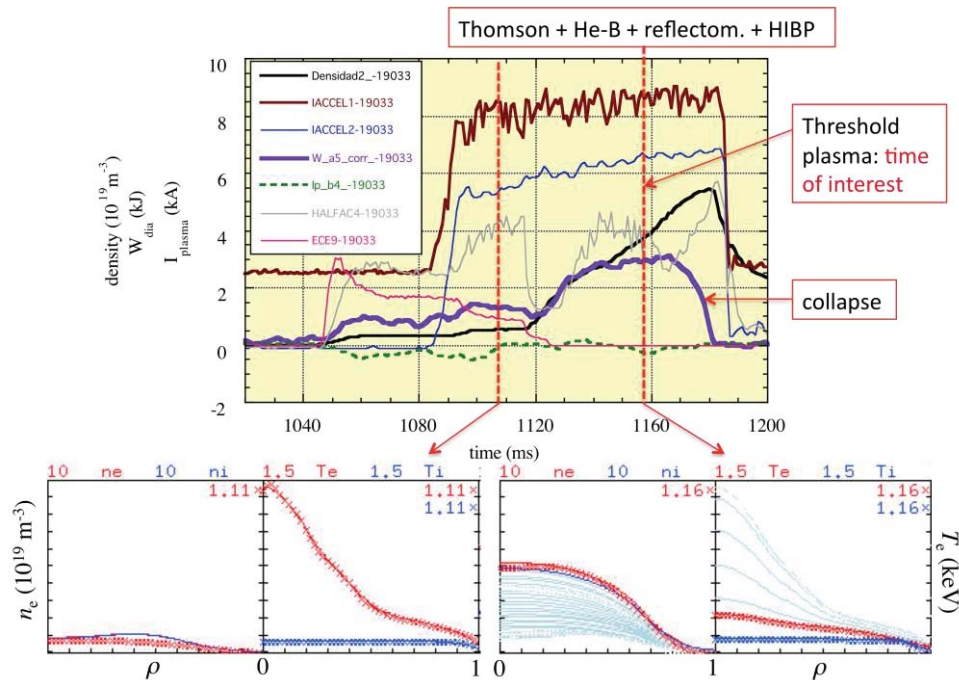


Figure 6. Time traces for balanced NBI discharge #19033. In arbitrary units: NBI currents (IACCEL), H α light near a limiter (HALFAC4) and core electron cyclotron emission (ECE9). Also shown are the line density, diamagnetic energy and net plasma current. The discharge undergoes a transition at $t \approx 1157$ ms (vertical dashed line) soon before radiative collapse. The bottom figures show the Astra [27] outputs for the experimental (crosses) and model (lines) density and temperature profiles at $t = 1115$ ms (bottom left) and at the transition threshold time (bottom right). Thin light lines in the bottom right figure show the calculated evolution from $t = 1115$ ms according to a transport model that reproduces the evolution of the line density.

The strong effect that magnetic resonances have on the access to/from H-mode plasma seems to stem from their effect on confinement already in L-mode conditions. TJ-II plasmas heated and fuelled by NBI show a different evolution during the L-mode and have different density thresholds depending on the presence or not of magnetic resonances near the plasma edge [26]. The upper plot in figure 6 represents time traces of several TJ-II diagnostics, like beam currents (IACCEL, a.u.) from the co- and counter-NBI systems, H α (HALFAC4, a.u.), and a central electron cyclotron emission signal (ECE9, a.u.) for TJ-II discharge #19033 with each NBI delivering around 0.45 MW (port-through power). In addition, the figure shows (left axis) line averaged density, diamagnetic energy and net plasma current. Note the very small values of the latter, from which we infer that the edge rotational transform must be very close to the vacuum one. Near $t = 1160$ ms there is an L-H transition, but it happens so close to the thermal collapse of the plasma that the increment in diamagnetic energy is barely notable.

Transport analysis is done in NBI discharges to study the evolution of the particle confinement time, τ_p , by means of a transport model in which the particle and energy sources are frequently updated. The bottom plots in figure 6 show the experimental profiles (crosses) and model calculations (lines) for the electron density. The temperatures for electron and proton species do not evolve from a model, but from diagnostic information (see [26] for details). The bottom right figure for the density also displays several lines in light color representing the evolution of the densities from the ECR phase to the L-H transition threshold. By reproducing the electron density evolution and checking for consistency with the diagnostics at the transition time (e.g. CX neutral particle fluxes), we obtain an estimate of the evolution of τ_p . The result is compared in figure 7 for discharges #19033 (figure 6) and #19065, which differ only on the edge rotational transform values: $\iota(a)/2\pi \approx 1.63$ and 1.61 respectively; i.e., the magnetic resonance 8/5 is placed around $\rho \approx 0.9$ in discharge #19033 but

practically at the plasma edge in discharge #19065. According to figure 7 the particle confinement time is smaller during the L-mode phase for the discharge that has the resonance *inside* the plasma (#19033). This discharge reaches the transition threshold at a smaller line density. According to the small plasma current and the balanced NBI scheme, the magnetic shear must be quite small, i.e., close to the vacuum shear, in these discharges. A study of how the radial electric field is modified by the presence of a magnetic resonance in NBI plasmas is underway. For now, we have identified notable changes in the density gradient region that, as mentioned, affect transition dynamics

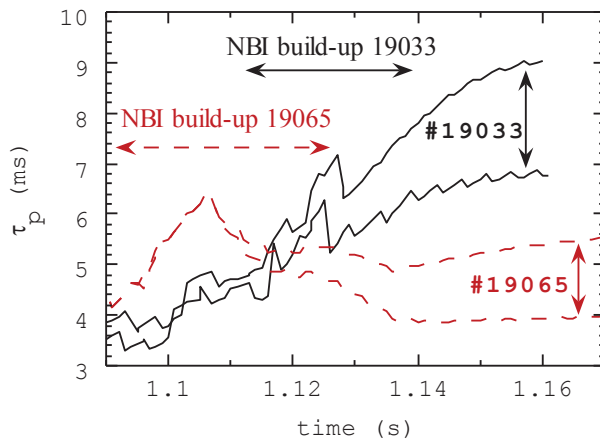


Figure 7. Calculated evolution of the electron confinement time for TJ-II discharges #19033 with $\iota(a) = 1.61$ (solid lines) and #19065 with $\iota(a) = 1.59$ (dashed lines). Two lines in each case delimit uncertainties in the calculations associated mainly with the edge temperatures.

We have mentioned a potential use of these findings for confinement control in a tokamak or stellarator reactor. Of course, our results cannot be extended beyond our plasma parameters. However, MHD dynamics in the TJ-II has been also studied keeping in mind a possible equal nature of tokamak and stellarator plasmas, particularly in matters concerning the effects of magnetic resonances on transport. At this respect, confinement events similar to tokamak phenomenology have been identified in TJ-II plasmas and related with MHD activity around the magnetic resonances [28]. In brief, and mostly based on the temporal and spatial resolution of bolometry diagnostics, magnetically resonant locations have been identified as well localized transport barriers (albeit weak) that can break suddenly causing sudden particle confinement losses. A repetitive breaking and restoration of confinement in the resonant regions provokes such events as sawteeth, internal crashes or ELM-like bursts. Up to now, an H-mode in the TJ-II looks like a state in which the barrier formed around the resonant region remains as such without subsequent failure.

3. Conclusions

In summary, the TJ-II experience is that the magnetic resonances provide another external knob because they—maybe their boundaries—modify significantly the radial fluxes and hence the plasma rotation in a local manner. This concept is quite old indeed, but we have provided a continued program to assess its practical implementation. Therefore, the notion of rarefaction of low order rational values of $\iota/2\pi$ may not imply that such magnetic resonances have to be avoided or allowed inside the plasma only with high magnetic shear. Good flux surfaces are desirable —this is not questioned at all— but isolated resonant locations, if “healed” or sufficiently narrow in minor radius extension, might become a necessary ingredient for transport and MHD control. At this respect, it is worth mentioning that a state of healed —not causing flattenings in plasma profiles— magnetic island associated to a major resonant surface is favored at *high plasma beta and low collisionality* in the LHD heliotron [29], the largest currentless magnetic confinement system to date. These are the conditions relevant for reactor plasmas.

Acknowledgments

All of the transport analyses presented here have been performed with the ASTRA transport shell [27]. This work is dedicated to the memory of G. V. Pereverzev.

References

- [1] *Proc. 3rd Int. Conf. on Plasma Physics and Controlled Nuclear Fusion Research* held by the IAEA at Novosibirsk, 1–7 August 1968, Vol. 1
- [2] Brakel R et al 1997 *Plasma Phys. Control. Fusion* **39** B273
- [3] Inagaki S et al 2004 *Phys. Rev. Lett.* **92** 055002
- [4] Castejón F et al 2004 *Nucl. Fusion* **44** 593
- [5] Yokoyama M et al 2007 *Nucl. Fusion* **47** 1213
- [6] Sano F et al 2005 *Nucl. Fusion* **45** 1557
- [7] Wagner F et al 2005 *Phys. Plasmas* **12** 072509
- [8] Estrada T et al 2010 *Contrib. Plasma Phys.* **50** 501
- [9] Austin M E et al 2006 *Phys. Plasmas* **13** 082502
- [10] Joffrin E et al 2002 *Plasma Phys. Control. Fusion* **44** 1739
- [11] Ascasíbar E et al 2002 *Plasma Phys. Control. Fusion* **44** B307
- [12] Vargas V I et al 2006 “Difusión térmica electrónica experimental en plasmas ECRH del TJ-II” [Informes Técnicos Ciemat 1079, Ciemat, Madrid, Spain, July 2006](#) (in Spanish)
- [13] Vargas V I et al 2007 *Nucl. Fusion* **47** 1367
- [14] Romero J A et al 2003 *Nucl. Fusion* **43** 387
- [15] López-Bruna D et al 2004 *Nucl. Fusion* **44** 645
- [16] López-Bruna D et al 2008 *Europhys. Lett.* **82** 65002
- [17] Ascasíbar E et al 2008 *Plasma Fusion Res.* **3** S1004
- [18] Romero J A et al 36th EPS Conference on Plasma Phys. Sofia, June 29 - July 3, 2009 [ECA Vol. 33E, P-4.183](#) (2009)
- [19] López-Bruna D et al 2009 *Nucl. Fusion* **49** 085016
- [20] López-Bruna D et al 2010 *Contrib. Plasma Phys.* **50** 600–604
- [21] Bondarenko O et al 2010 *Contrib. Plasma Phys.* **50** 605–609
- [22] Pedrosa M A et al [3rd EFDA Transport Topical Group Meeting & 15th EU-US Transport Task Force Meeting, Córdoba, Spain, September 7–10, 2010](#)
- [23] López-Bruna D et al 2011 *Plasma Phys. Control. Fusion* **53** 124022
- [24] Estrada T et al 2009 *Plasma Phys. Control. Fusion* **51** 124015
- [25] Romero J A et al 2012 *Nucl. Fusion* **52** 023019
- [26] López-Bruna D et al 2013 *Plasma Phys. Control. Fusion* **55** 015001
- [27] Pereverzev G V and Yushmanov P N 2002 “ASTRA: Automated System for TRansport Analysis,” Tech. Rep. IPP 5/98, Max Plank Institut für Plasmaphysik, Garching, February 2002
- [28] López-Bruna D et al 2013 *Nucl. Fusion* **53** 073051
- [29] Narushima Y et al 2008 *Nucl. Fusion* **48** 075010